NACA RM L53H07

NACA

RESEARCH MEMORANDUM

AN EXPERIMENTAL STUDY OF POROSITY CHARACTERISTICS OF PERFORATED MATERIALS IN NORMAL AND PARALLEL FLOW

By George M. Stokes, Don D. Davis, Jr.,
and Thomas B. Sellers

Langley Aeronautical Laboratory
Langley Field, Va.

NATIONAL ADVISORY COMMITTEE
FOR AERONAUTICS

WASHINGTON

November 10, 1953

NATIONAL ADVISORY COMMITTEE FOR AERONAUTICS

RESEARCH MEMORANDUM

AN EXPERIMENTAL STUDY OF POROSITY CHARACTERISTICS OF PERFORATED MATERIALS IN NORMAL AND PARALLEL FLOW

By George M. Stokes, Don D. Davis, Jr., and Thomas B. Sellers

SUMMARY

An experimental investigation was conducted in order to determine the porosity characteristics of perforated materials for normal and parallel flow. The results of the normal-flow test showed that the porosity of the material is governed principally by its open ratio, but that density has a slight effect. When the same material was tested under parallel-flow conditions, the effective porosity dropped markedly as the stream velocity increased.

A new definition is given which permits the concept of a discharge coefficient to be extended to the case of parallel flow. An essential feature of this extension is that the discharge coefficient is based on the total velocity in the discharge jet rather than on some velocity component normal to the wall. Discharge coefficients were determined for the test materials for parallel-flow stream velocities ranging from 200 to 1,400 fps. The most important parameter in determining the discharge coefficient of the material was found to be the ratio of the stream velocity to the jet velocity. For the same velocity ratios, the discharge coefficients at the supersonic velocity tested were less than those for the subsonic velocities tested.

INTRODUCTION

In recent years there has been increased interest in the use of perforated materials for solving certain aerodynamic-flow problems. Efforts are now being made to obtain satisfactory wind-tunnel walls and supersonic diffusers (ref. 1) through the use of perforated materials.

These applications require the perforated material to operate in a fluid having its major velocity component in a plane parallel to that of the material.

Since the porosity characteristics of the material must be such that a desired outflow will be provided with a given pressure drop, information is needed to show how a proper wall selection can be made. Although some limited information is available for normal flow, no such information is available for the parallel-flow condition. Consequently, this investigation was conducted in order to determine some of the flow characteristics of perforated materials and to establish which quantities are of most importance in determining the porosity characteristics of perforated materials.

SYMBOLS

A_h	width of two-dimensional opening
A_j	width of two-dimensional jet
M	free-stream Mach number
m_n	mass flow per unit area through perforated material
P_j	static pressure beneath opening
P_s	static pressure in stream
r_o	open ratio, ratio of open area of perforated material to total area of material
u/V_s	ratio of velocity at point in boundary layer to free-stream velocity
V_j	jet velocity, velocity corresponding to total-pressure difference across material
V_n	component of velocity normal to porous material, m_n/ρ_s, fps
V_s	stream velocity, velocity component parallel to porous material, fps
ΔP	static-pressure drop across perforated material, $P_s - P_j$, lb/sq ft
ρ_j	density of fluid in jet, slugs/cu ft

ρ_s density of fluid before entering perforated material, slugs/cu ft

σ discharge coefficient, ratio of jet minimum area to hole area; in general, $\sigma = \frac{m_n}{\rho_j V_j r_o}$ and, for the special case of normal flow, the approximate incompressible-flow equation $\sigma = \frac{V_n}{r_o}\sqrt{\frac{\rho_s}{2\Delta P}}$ is used

ANALYSIS

The determination of the relationship between the pressure drop across a perforated wall and the flow through the wall in the presence of a component of the stream velocity which is parallel to the wall presents a difficult analytical problem. However, some insight into the nature of the flow and the parameters which control the flow may be obtained by a study of the two-dimensional, nonviscous, incompressible flow through an opening in a thin wall:

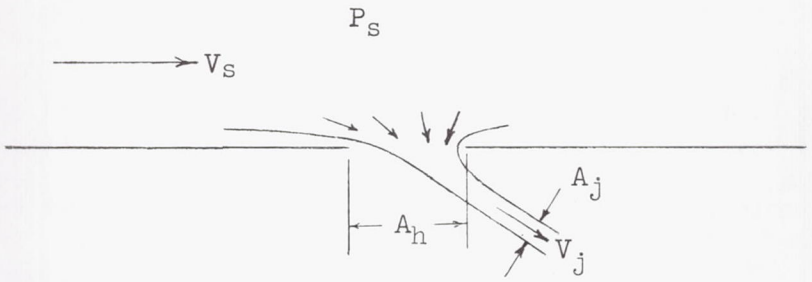

In parallel flow, as in normal flow, the flow is expected to issue from the opening in the form of a jet of fluid. The free streamlines at the outer edges of the jet are at a constant pressure and, therefore, at a constant velocity. If the stagnation pressure and temperature in the free stream are known, and if the pressure beneath the opening is known, the velocity V_j can be calculated. In order to determine the flow through the opening, the only further quantity required is the width of the jet beneath the opening.

The problem presented by the type of flow shown in the preceding sketch has been solved in reference 2 in connection with the design of free streamline suction slots. The ratio of jet width to open width is found to be a function of the exit velocity ratio V_s/V_j alone.

For normal flow ($V_s = 0$), the discharge coefficient is defined as the ratio of the jet area to the open area. By an extension of this definition, the ratio of jet area to open area in the parallel-flow case ($V_s > 0$) will be defined here as the discharge coefficient for parallel flow. It is important to note that this discharge coefficient is related to the total velocity V_j rather than to the velocity component which is normal to the wall. It is evident that, as the rate of outflow through the opening is reduced, the jet will be inclined toward the wall until in the limit, as the outflow approaches zero and V_j approaches V_s, the jet will be parallel to the wall and the jet width will be zero. Thus, it is inherent in the nature of the preceding definition for the discharge coefficient that, as the outflow approaches zero in the parallel-flow case, the discharge coefficient will also approach zero. Conversely, if the stream velocity is increased, with the outflow held constant, the discharge coefficient will be reduced. As V_s/V_j increases from 0 to 1, the discharge coefficient decreases from the normal-flow value to zero. At a given fixed value (other than zero) of the free-stream velocity, if a very small quantity of flow is removed through the opening, the discharge coefficient will be very small, but, as the jet velocity V_j is increased, the discharge coefficient will also increase.

These results for two-dimensional, nonviscous, incompressible flow give some insight into the probable nature of the outflow through a perforated wall. The discharge coefficient would be expected to be lower for parallel flow than for normal flow. Furthermore, the exit velocity ratio would be expected to be the primary parameter controlling the magnitude of the discharge coefficient.

Although the nature of this flow dictates that the discharge coefficient be related to the jet velocity, the designer in most cases will be interested primarily in the average velocity normal to the wall. For a perforated wall, the relationship between this outflow velocity and the pressure drop is regarded as the "effective porosity" of the wall. Thus, it is of interest to determine how the static-pressure drop required to obtain a fixed outflow is affected by an increase in the stream velocity. An analysis of this problem, based on the two-dimensional theory, shows that the required pressure drop increases rapidly as the stream velocity is increased. Thus, an increase in the stream velocity would be expected to result in a decrease in the effective porosity of a perforated wall.

Because the thickness of most commercial perforated materials is of the same order of magnitude as the hole diameter, the walls cannot actually be considered to be infinitely thin, as was the case in the preceding analysis. The actual flow pattern is probably similar to that indicated in the following sketch:

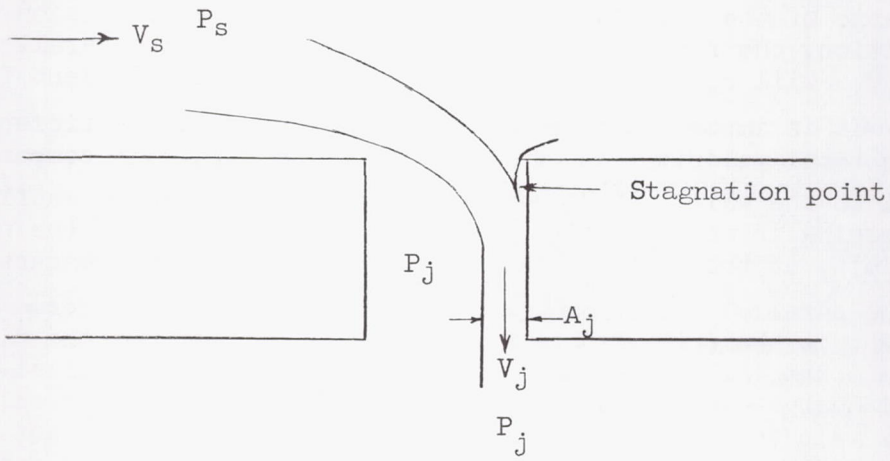

With this type of flow, the discharge coefficient will again be a function of V_s/V_j and the effect of parallel flow on the effective porosity will be qualitatively similar to the effect found in the analysis of the thin wall.

APPARATUS

The porous material used for making these tests was a 2-inch-square piece of 0.035-inch-thick Plexiglas. The Plexiglas was bonded to a supporting base made of 1/2-inch lengths of 0.060-inch outside-diameter and 0.050-inch inside-diameter Monel tubing stacked parallel and bonded together as closely as possible. The Plexiglas top was made porous by drilling small holes over the centers of the 0.050-inch holes in the supporting base. Figure 1 shows a photograph of this perforated material mounted in its test block. The porosity of the material was changed by redrilling the holes in the Plexiglas top to successively larger diameters, the number of holes being kept constant. The diameters of the holes tested were 0.0190, 0.0247, 0.0260, 0.0287, 0.0360, and 0.0390 inch. These values were obtained by measuring several of the hole diameters to the nearest 0.0002 inch and by taking the average. The base of the Monel tubing was used principally to provide a rigid backing for the 2-inch-square porous surface and to prevent cross flow under the sample.

Figure 2 is a schematic drawing of the arrangement of equipment used for making normal-flow tests. The two flow meters used were the Fischer and Porter Flowrator type having ranges from 6 to 60 and 50 to 300 cu ft/min. The settling chamber was constructed so that uniform flow was induced in the 3- by 5.8-inch section just ahead of the porous material.

An aircraft supercharger furnished the suction required for the experiments. Figure 3 is a photograph of the complete normal-flow test apparatus.

A 3-inch-square supersonic tunnel designed for a Mach number of 1.3 was used for making parallel-flow measurements. This tunnel was originally designed to have porous walls installed just to the rear of the supersonic nozzle in order to study wave-reflection problems. For these tests, however, the bottom porous wall was removed and the 2-inch-square perforated material was installed in its place. The air exhausted through the perforated material was drawn into a metering line, incorporating a settling chamber and flow meter. It then joined the air exhausted through the top porous wall before entering the suction supply. Figure 4 shows a schematic drawing of the parallel-flow test configuration. Figure 5 is a photograph of the porous material mounted in the test section.

TESTS

Normal-flow tests were made for six different open ratios of 0.087, 0.148, 0.163, 0.200, 0.315, and 0.365. The basic measurements taken were those of pressure drop across the material, mass flow through the material, and air temperature and pressure before entering the material.

Parallel-flow measurements were made for the four open ratios of 0.148, 0.200, 0.315, and 0.365. The measurements taken were the same as those for normal flow in addition to the stagnation and static pressure of the parallel flow. Data were obtained for the approximate parallel-flow Mach numbers of 0.2, 0.4, 0.6, 0.8, and 1.3 for each open ratio.

Boundary-layer surveys were made at 0.06 inch ahead and 1.87 inches behind the upstream edge of the 36.5-percent open porous material at a Mach number of 1.3.

RESULTS AND DISCUSSION

Normal Flow

The results of the normal-flow tests are presented in figures 6 to 9. Figures 6 and 7 show graphically the manner in which the velocity normal to the perforated material varies with the ratio $\Delta P/\rho_s$ for two different values of ρ_s. The fact that the curves for equal open ratios are not identical indicates that there is some change in the porosity characteristics due to a variation in ρ_s. Reading the slopes of the curves

from the logarithmic plots shows that the pressure drop varies approximately with the velocity squared.

A careful analysis of the data on the basis of Reynolds number (based on hole diameter) showed that the discharge coefficient was approximately constant for the high Reynolds numbers tested but dropped off for low Reynolds numbers. These results are consistent with those shown for nozzles in reference 3. The Reynolds numbers at which the discharge coefficients for the data presented in this paper began to drop off will be called the "tolerance limit" to be consistent with data shown in reference 3. When the velocity used for evaluating the Reynolds number exceeded a Mach number of approximately 0.4, the discharge coefficients began to drop, thus indicating an effect of compressibility. The slope changes found in each curve describing the porosity characteristics of the material (figs. 6 and 7) are results of the changing discharge coefficients. The calibrations at the higher density (fig. 7) do not reflect the Reynolds number and Mach number effects as noticeably as those at the low density because of the change in range of flow conditions tested.

In order to show a general effect of density on the discharge coefficient, an average of coefficients for each calibration shown in figures 6 and 7 was taken and plotted in figure 8. These curves show that the density has a definite effect on the discharge coefficient, in addition to showing that there is no appreciable change in the discharge coefficient as a result of changing the open ratio or hole diameter for the range investigated. Since this density effect was unexpected, the basic data were carefully checked. No reason was found to doubt the existence of the density effect shown. The density effect was found to be constant with changes in Reynolds number and Mach number, provided the Reynolds number was greater than the tolerance limit and the Mach number was less than 0.4.

Some of the data of figure 6 have been cross-plotted to form figure 9 which shows that the normal velocity is a linear function of the wall open ratio. Since the data for these curves were obtained from materials whose hole diameters varied by a ratio of greater than 2 to 1, and, since no slope changes are shown in the curves, as would be expected if the hole diameters had an effect, it is reasoned that the hole diameter had little or no effect in determining the porosity characteristics of the material tested. These facts are significant in that they show that it is possible to predict the porosity characteristics of a given material if the open ratio is known. These results are valid within the range of flow variables used to obtain the data in figure 9. If a similar cross plot were made by using the high-density data, the slopes of these curves would increase; this result is consistent with the results shown in figure 8.

To summarize, the results of the normal-flow test show that (1) the pressure drop across the porous material varies approximately with the velocity squared, (2) the discharge coefficient appears to be a function of density, and (3) when considering small changes in hole diameter, the porosity characteristics are a function of the open ratio of the material and not a function of the hole diameter, provided the Reynolds number range does not fall below the tolerance limit and compressibility effects are not encountered.

Parallel Flow

Results showing the characteristic behavior of the perforated wall in parallel flow may be found in figures 10 to 12. A comparison of the curves in figure 10 with those of figure 6 shows that the effective porosity of the material at $M = 1.3$ has dropped markedly below that for a normal-flow condition. This phenomenon, however, is not surprising, since the two-dimensional analysis previously discussed indicated that such an effect might exist. No effort was made to compute the degree of the porosity drop in parallel flow on a theoretical basis, since the influence of such factors as boundary layer, hole depth, and jet mixing could not be determined. The slopes of the curves describing the parallel-flow characteristics were found to fall off with increases in the parallel-flow velocity so that, when a Mach number of 1.3 is reached, the power to which the velocity affects the pressure drop is approximately 1.3. This fact is of considerable importance when dealing with problems concerned with the selection of a wall for the reduction of shock-wave reflections.

In order to show more graphically how parallel-flow velocity past the perforated material varies the pressure-drop characteristics, figure 11 is presented for four open ratios and for an outflow velocity V_n of 30 fps. Although the trends of the curves are similar in that a progressively increased pressure-density ratio $\Delta P/\rho_s$ is required as stream velocity increases, severe losses in the holes are indicated for the low open ratio requiring a very large increase in pressure to maintain a constant outflow. For example, for a constant pressure-density ratio of 40×10^3 and a constant normal velocity of 30 fps, it is found in the normal-flow curves of figure 9 that an open ratio of about 12 percent is required. For the same conditions, the wall in parallel flow is required to be about 15 percent open at 100 fps stream velocity or about 30 percent open at $V_s = 900$ fps. The theoretical consideration previously discussed indicated that this type of phenomenon should occur. The curves have been dashed in the transonic-speed range in order to indicate that there may be some porosity behavior different from that shown by the curve fairings. Limitations of the test equipment prevented data from being taken through this transonic range.

The characteristic curves of figure 12 describe more fully the performance of perforated walls. These plots show the manner in which the discharge coefficient σ varies with the velocity ratio V_s/V_j. Close inspection of the curves shows that there is practically no difference in the general porosity characteristics for the open ratios of 0.148, 0.200, and 0.315. The largest ratio, 0.365, differs from the others only in that it has a slightly increased discharge coefficient in subsonic flow.

The jet velocity V_j for these plots was determined by taking the ratio of the static pressure below the wall and the stream total pressure and computing the Mach number and local speed of sound on the basis of isentropic flow. It should be understood that this method of treatment is exact only for thin walls; consequently, allowances must be made when the hole depth exceeds some length which causes the pressure at the top of the hole to differ greatly from that at the bottom.

Curves such as these describing the characteristics of perforated materials in parallel flow are of considerable aid to the designer who desires to select a material having certain porosity characteristics for a given set of conditions. For instance, the wind-tunnel designer may desire a wall to have a certain outflow velocity V_n with a specific pressure drop. By using the stream Mach number, temperature, and total pressure, along with the desired value of ΔP, a theoretical jet velocity V_j and stream velocity can be computed. With the computed value of V_s/V_j, the discharge coefficient of the material for the particular stream condition can be read from the parallel-flow-characteristics curve of figure 12. The open ratio r_o may now be computed from the expression

$$r_o = \frac{\rho_s V_n}{\rho_j V_j \sigma}$$

In the event that a designer must use a material that differs greatly in thickness and hole diameter from the material used in these calibrations, the results presented may not enable him to predict exactly the characteristics of the material but they will afford a first approximation. For precision, the material selected on the basis of this first approximation should be calibrated and a curve similar to the curves of figure 12 should be prepared for use in the next approximation. Good results should be obtained by using this technique for wall selection.

Boundary Layer

Velocity profiles of the boundary layer for two suction conditions are shown in figure 13. These data were taken for the material having an open ratio of 0.365 (0.039-inch-diameter holes) at a Mach number of 1.3. An inspection of these data indicates two results: (1) for no suction (zero pressure difference), boundary-layer displacement thickness decreases and (2) an almost complete bleeding of boundary layer from the test specimen occurs when a pressure difference of 120 lb/sq ft is applied. A comparison of the two lower curves of figure 13 for zero pressure difference indicates that the boundary-layer velocity increases rapidly over the perforated section. The fact that the boundary-layer displacement thickness appears to be less at the 1.87-inch downstream station over the porous material than for the more forward station for no suction indicates that there may have been some outflow through the material. Although the static pressure below the material was set equal to the free-stream static pressure, a portion of stream total pressure could have been recovered in the localized positions of the individual holes and caused some of the boundary layer to move through the holes, thus accounting for the reduction in boundary-layer thickness. The curve obtained when suction is applied reveals the rapidity with which the boundary-layer thickness reduces. Although no data were taken at a station just behind the first few rows of holes to determine the boundary-layer displacement thickness at this point, it is conceivable that the boundary layer becomes very thin just downstream of the initial outflow station. These boundary-layer profiles are presented principally to give the reader some idea about the type of flow existing immediately over the porous material.

CONCLUSIONS

Results from an experimental investigation to determine the porosity characteristics of perforated materials for normal and parallel flow indicate the following conclusions:

1. Within certain tolerance limits of Reynolds number and Mach number, the pressure drop through a perforated material in normal flow varies approximately with the second power of velocity normal to porous material V_n. In parallel flow at a Mach number of 1.3, the pressure drop varies approximately with the 1.3 power of V_n.

2. The open ratio is the important factor in determining the porosity characteristics for materials in normal flow. The hole diameter has little or no effect on the porosity characteristics in the ranges of variables tested.

3. Lowering the density of the fluid over the perforated material causes a small drop in the normal-flow discharge coefficient.

4. The pressure difference required to obtain a given constant outflow increases rapidly as the parallel-flow velocity is increased.

5. The primary parameter governing the discharge coefficient of the perforated material in parallel flow is the ratio of stream velocity to jet velocity V_s/V_j.

6. Curves described by plotting the discharge coefficient against V_s/V_j can be used to select a porous material having certain desired porosity characteristics.

Langley Aeronautical Laboratory,
National Advisory Committee for Aeronautics,
Langley Field, Va., August 4, 1953.

REFERENCES

1. Evvard, John C., and Blakey, John W.: The Use of Perforated Inlets for Efficient Supersonic Diffusion. NACA RM E51B10, 1951.

2. Watson, E. J.: Free Streamline Suction Slots. R. & M. No. 2177, British A.R.C., 1946.

3. Anon.: Standards for Discharge Measurement With Standardized Nozzles and Orifices. NACA TM 952, 1940.

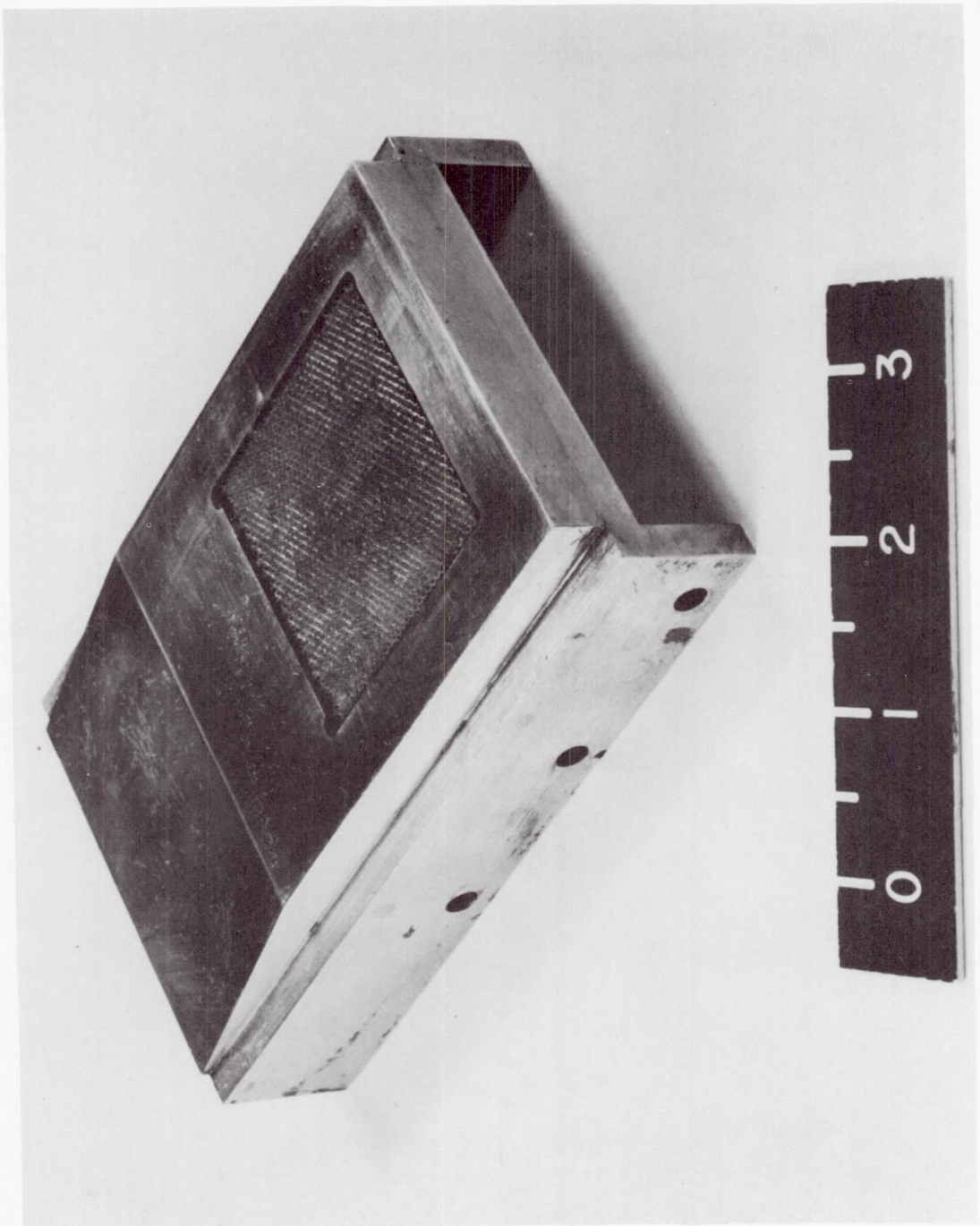

L-79404

Figure 1.- Perforated material mounted in test block.

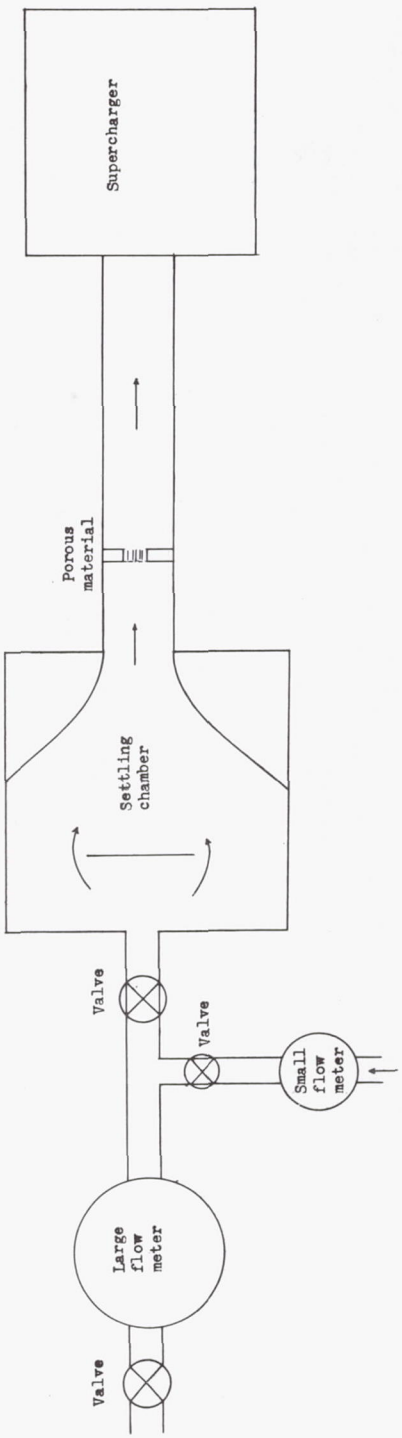

Figure 2.- Schematic diagram of normal-flow test setup.

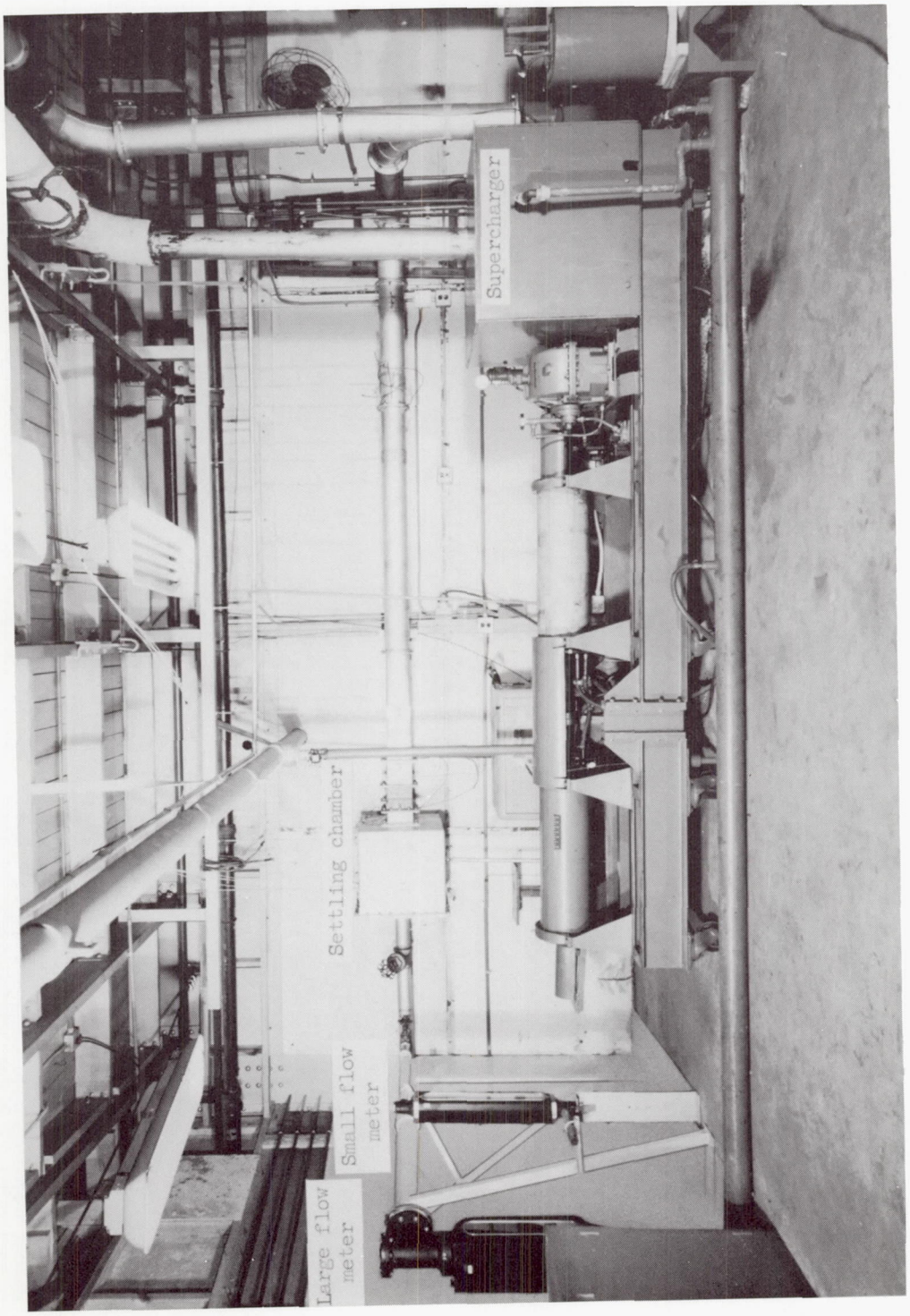

L-79395.2

Figure 3.- Normal-flow test apparatus.

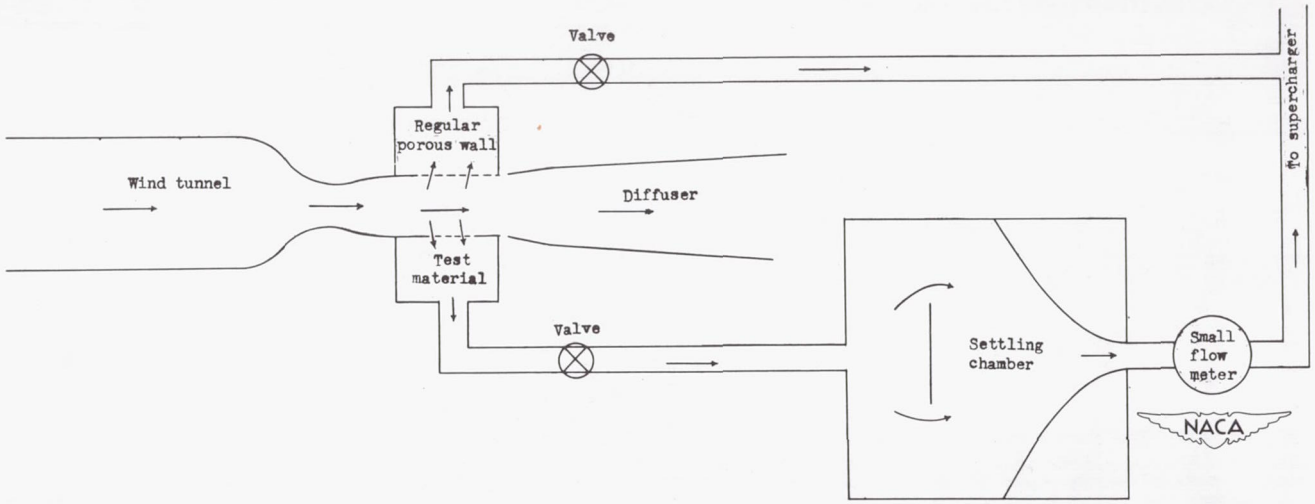

Figure 4.- Schematic diagram of parallel-flow test setup.

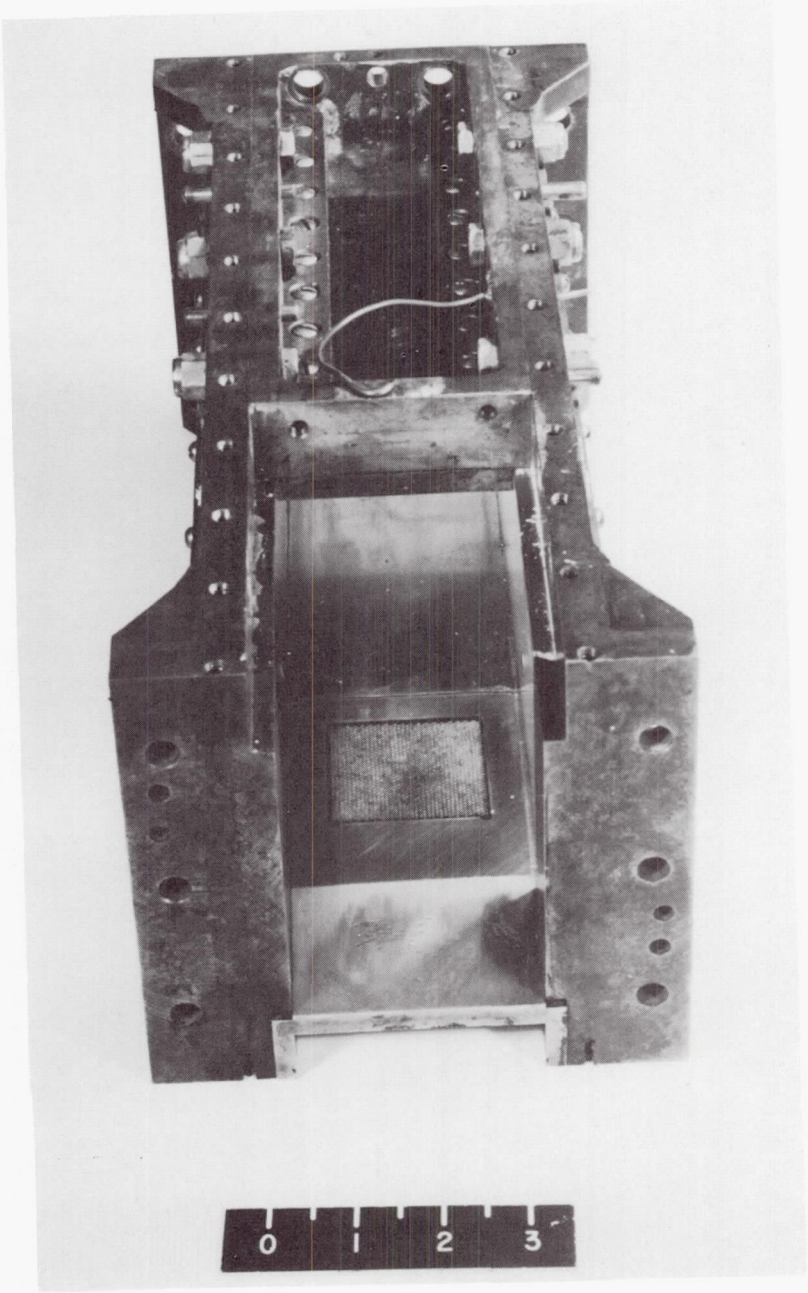

L-79405

Figure 5.- Porous material mounted in tunnel in place of regular wall section.

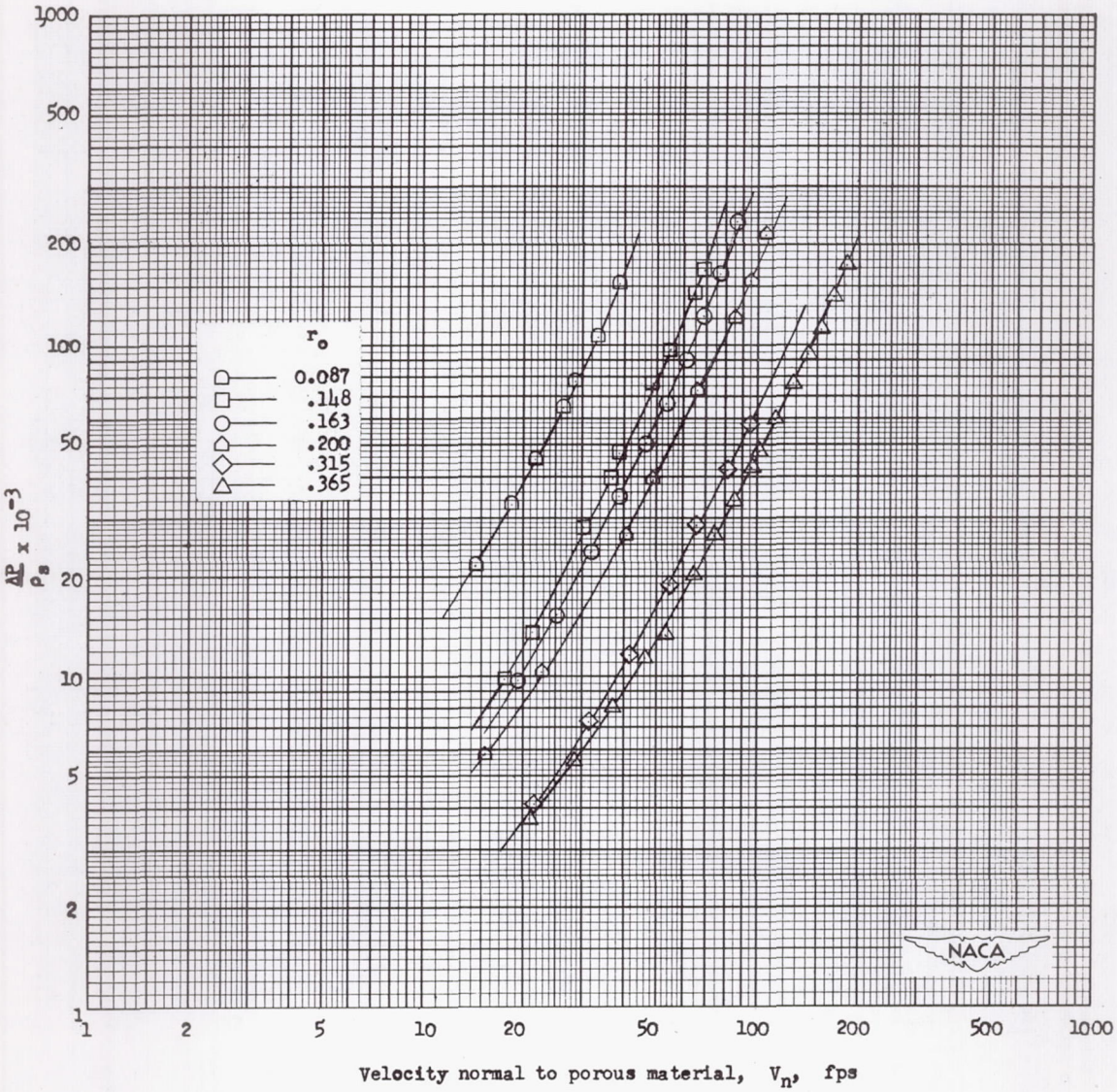

Figure 6.- Normal-flow calibration of perforated material for several different open ratios. $\rho_s \approx 0.0009$ slugs/cu ft.

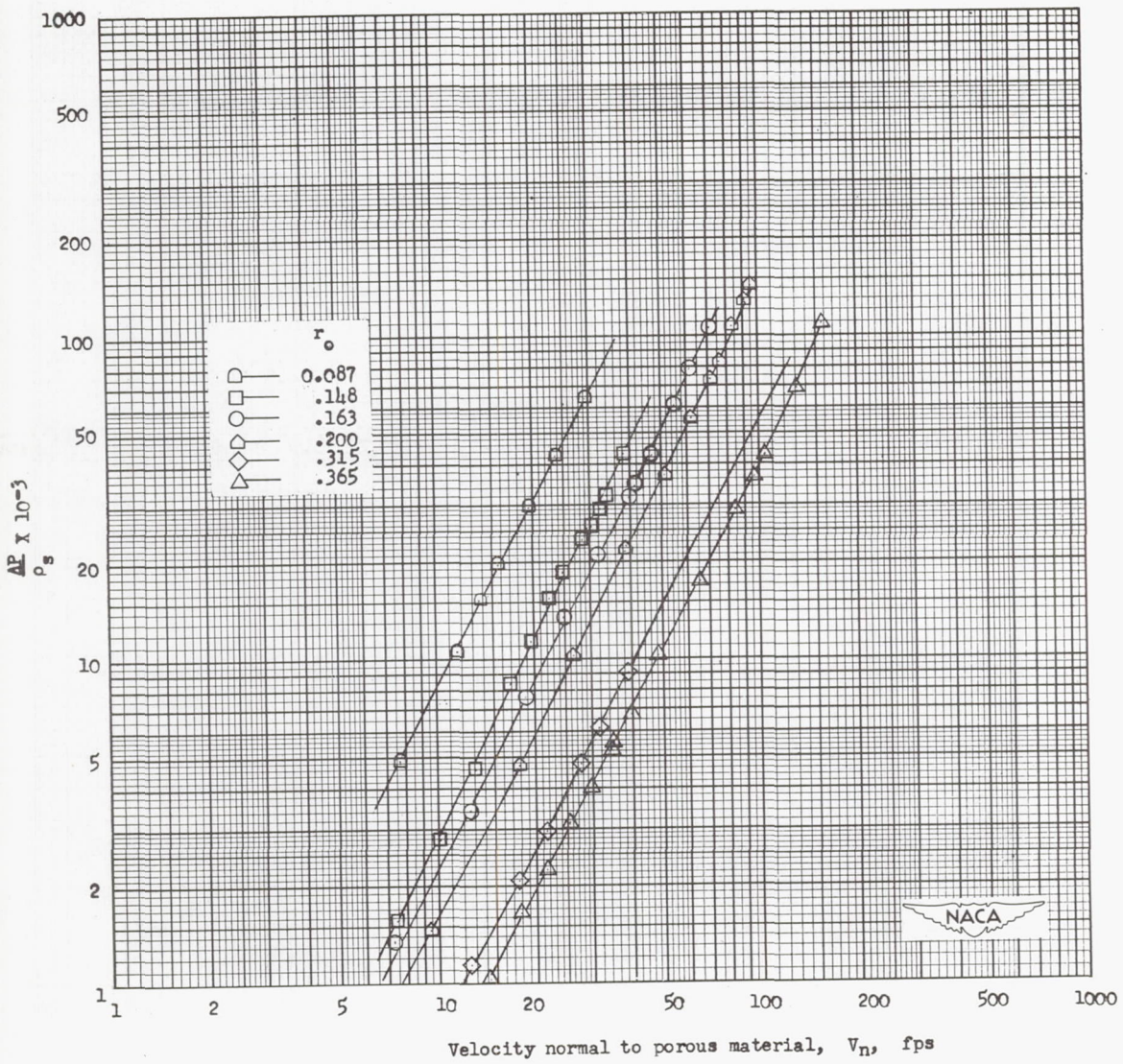

Figure 7.- Normal-flow calibration of perforated material for several different open ratios at a density approximately equal to 0.0022 slugs/cu ft.

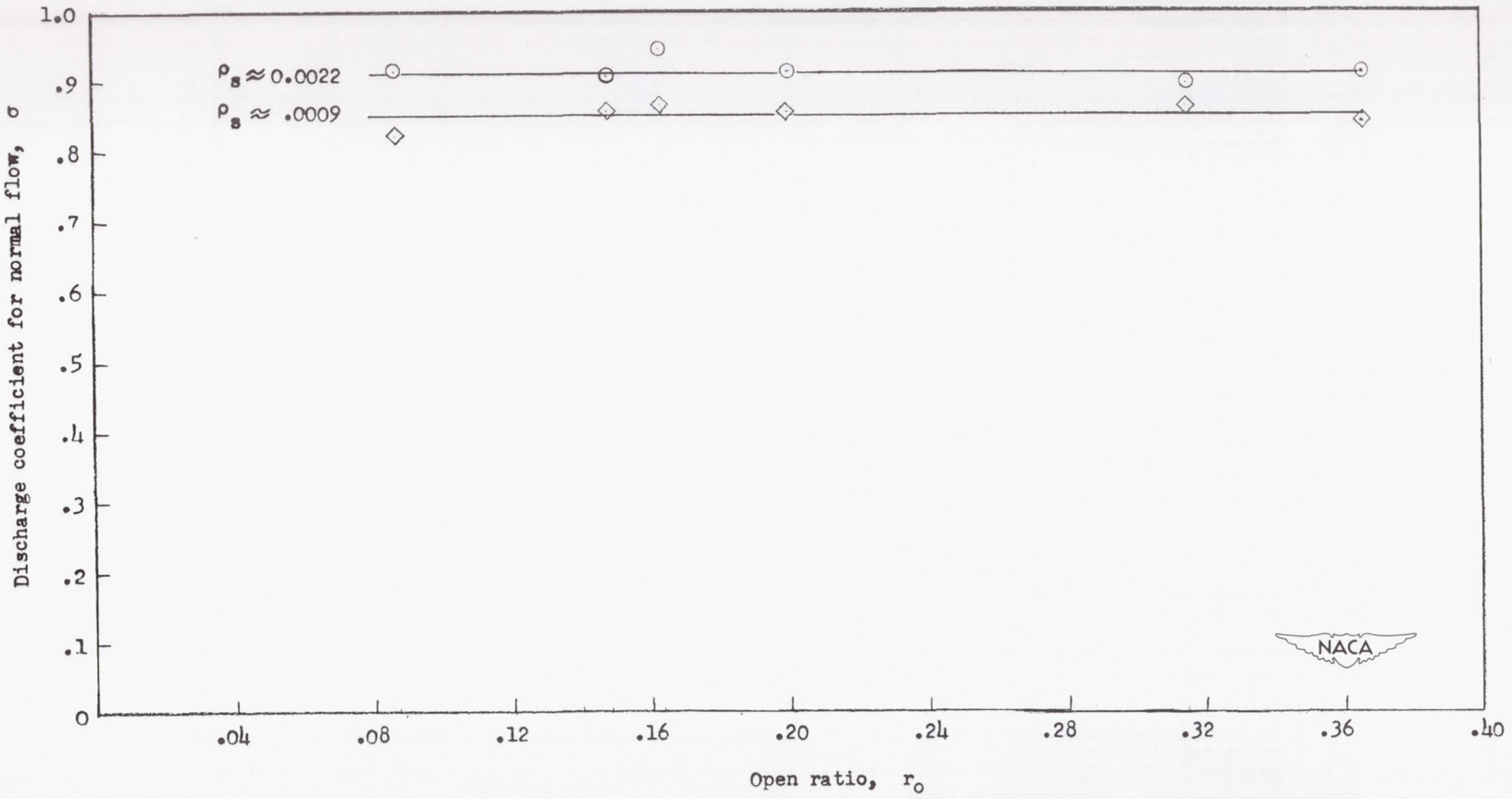

Figure 8.- Comparison of discharge coefficients for two different densities.

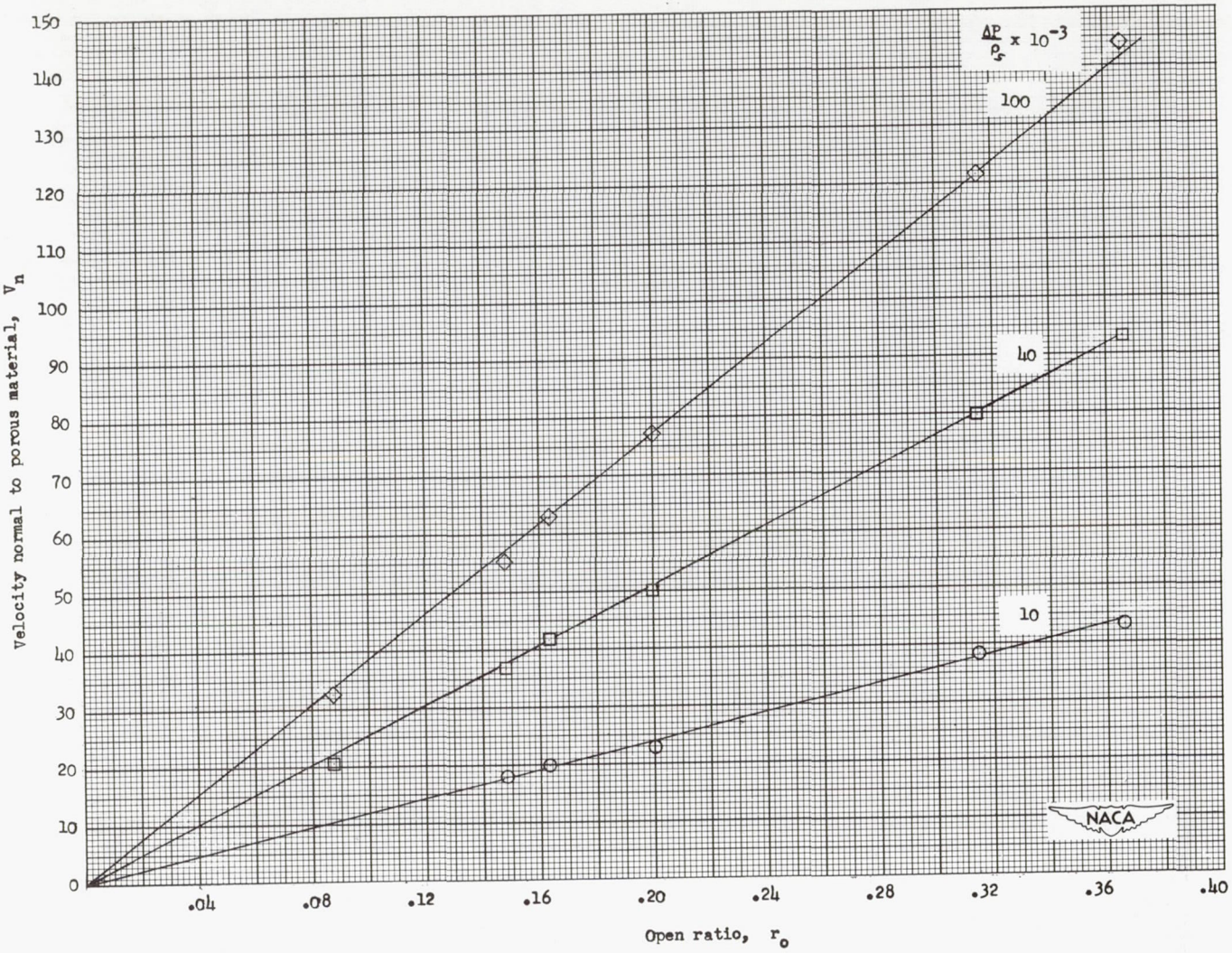

Figure 9.- Cross plots showing relationship between open ratio and velocity normal to porous material for three different $\Delta P/\rho_S$ ratios. $\rho_S \approx 0.0009$.

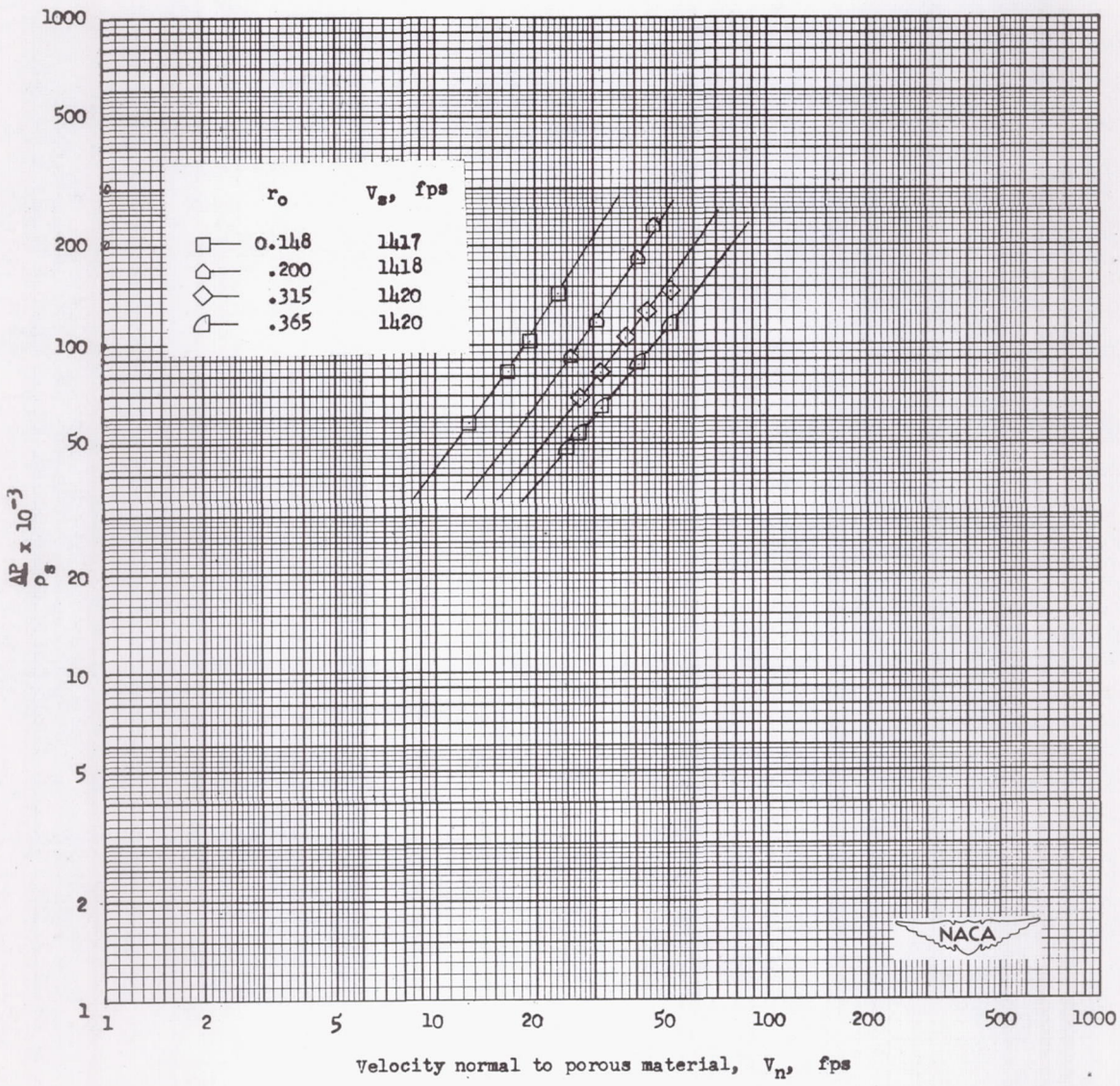

Figure 10.- Parallel-flow calibrations of four different open ratios in porous material at a Mach number of approximately 1.3. $\rho_s \approx 0.0009$.

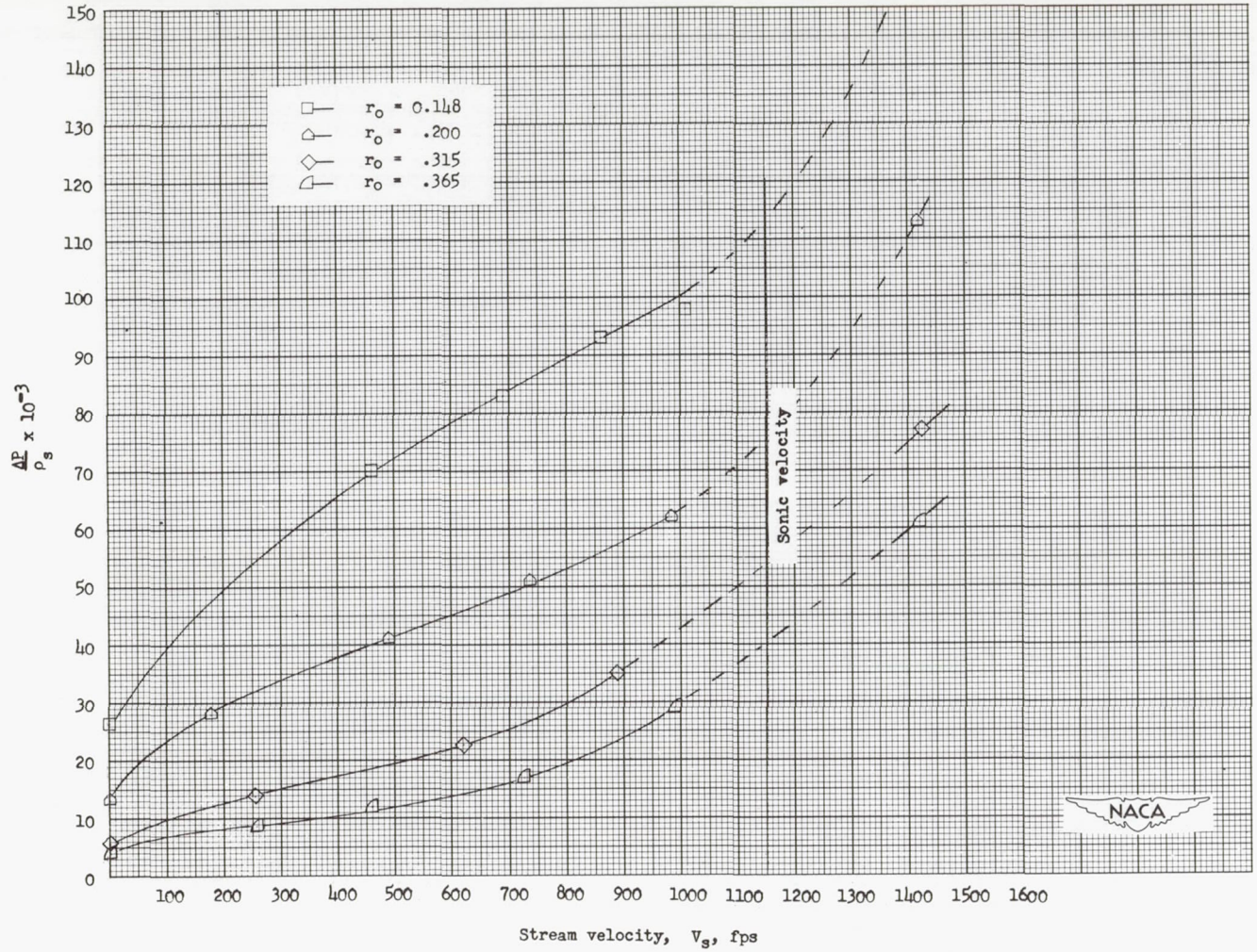

Figure 11.- Curves showing the manner in which $\Delta P/\rho_s$ varies with parallel-flow stream velocity for four porous-material open ratios with a constant normal velocity of 30 fps. Symbols indicate cross-plot points.

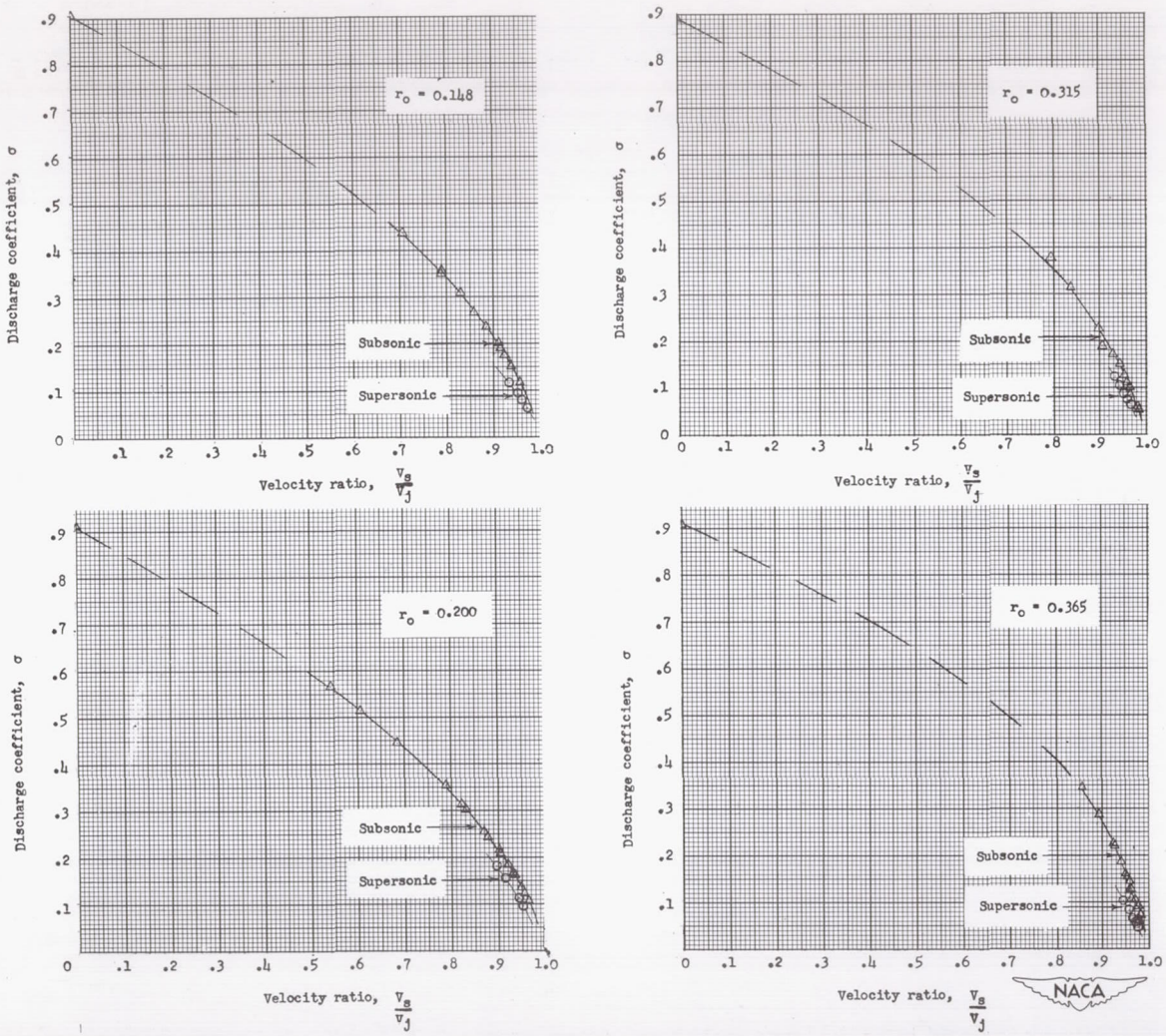

Figure 12.- Relation between discharge coefficient and velocity ratio for porous material in parallel flow.

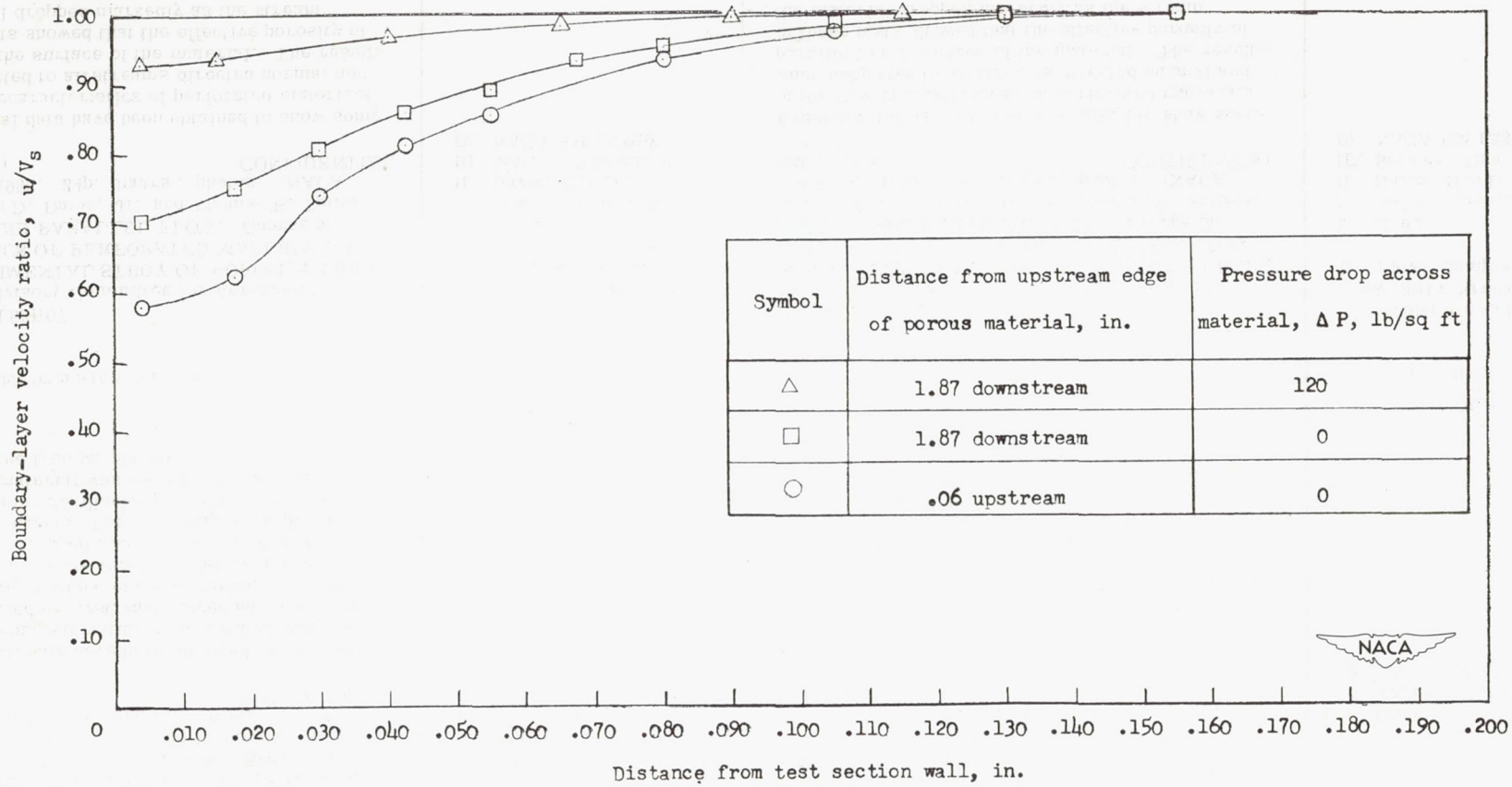

Symbol	Distance from upstream edge of porous material, in.	Pressure drop across material, Δ P, lb/sq ft
△	1.87 downstream	120
□	1.87 downstream	0
○	.06 upstream	0

Figure 13.- Boundary-layer velocity profiles of flow just ahead and over porous material at a Mach number of 1.3. $r_o = 0.365$.

NACA-Langley - 11-10-53 - 325